AIAA Meeting Papers on Disc, 1996, pp. 224-232
A9634736, AIAA Paper 96-3597

The effect of parameter uncertainties on the aerobraking tether

Steven G. Tragesser
Purdue Univ., West Lafayette, IN

James M. Longuski
Purdue Univ., West Lafayette, IN

AIAA/AAS Astrodynamics Conference, San Diego, CA, July 29-31, 1996, Collection of Technical Papers (A96-34712 09-12), Reston, VA, American Institute of Aeronautics and Astronautics, 1996, p. 224-232

A sensitivity analysis of the aerobraking tether is performed. Perturbations of the input variables are simulated to understand how uncertainty in the atmosphere and in the initial conditions affect the fly-through maneuver. These preliminary results indicate relative insensitivity of the final orbit. A redesign of the tether is then performed so that it can accommodate the parametric uncertainties without violating the constraints by breaking or compressing the tether, subjecting the orbiter to atmospheric effects, crashing the spacecraft, or failing to capture. The system is then evaluated using Monte Carlo simulation to show that the additional (rotational) degree of freedom makes the tethered system more robust (in terms of final eccentricity) than a conventional ballistic vehicle. (Author)

AIAA-96-3597-CP

THE EFFECT OF PARAMETER UNCERTAINTIES ON THE AEROBRAKING TETHER

Steven G. Tragesser * and James M. Longuski†
Purdue University, West Lafayette, IN 47907-1282

Abstract

A sensitivity analysis of the aerobraking tether is performed. Perturbations of the input variables are simulated to understand how uncertainty in the atmosphere and in the initial conditions affect the flythrough maneuver. These preliminary results indicate relative insensitivity of the final orbit. A redesign of the tether is then performed so that it can accommodate the parametric uncertainties without violating the constraints by: breaking or compressing the tether, subjecting the orbiter to atmospheric effects, crashing the spacecraft or failing to capture. The system is then evaluated using Monte Carlo simulation to show that the additional (rotational) degree of freedom makes the tethered system more robust (in terms of final eccentricity) than a conventional ballistic vehicle.

Introduction

A great deal of research has been focused on using aerobraking vehicles as a cost-effective means of deceleration, particularly at Mars. Unfortunately, large variations in the predicted density of the Martian atmosphere can be expected due to lack of data and short period phenomena such as dust storms.[1,2] This uncertainty in the characterization of the atmosphere may cause large errors in the orbit achieved by a ballistic vehicle. One way to decrease the sensitivity of the problem is to use propellant to achieve capture and then use aerobraking over multiple passes to circularize the orbit.[3] Another option is to employ a feedback control scheme on a lifting body that can adjust the angle of attack for the variations encountered.[4-6] This paper explores a third option, the aerobraking tether.

Unlike a conventional ballistic vehicle, the aerobraking tether, shown in Fig. 1, requires only a portion of the spacecraft to be subjected to aerodynamic drag (the probe) while the other vehicle (the orbiter) is kept outside the atmosphere by the use of a long, thin tether. Before entering the atmosphere, the tether system spins in the orbital plane opposite to the orbital motion as in Fig. 2. During the atmospheric flythrough, the torque caused by the drag acting on the probe slows the spin rate to zero, after which the tether spins up in the opposite direction.

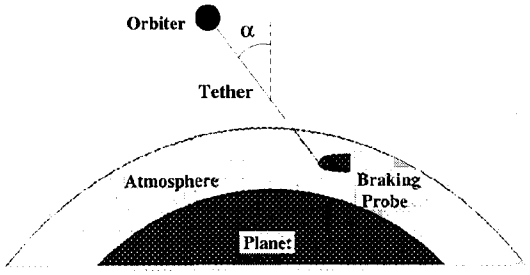

Fig. 1 Aerobraking tether.

Under nominal conditions, the system has been theoretically demonstrated to adequately achieve acrocapture.[7-11] The next step in the feasibility analysis is to consider the effect of parameter uncertainties on the aerobraking tether. Our purpose in this paper is to investigate whether the system has any robustness advantages over a conventional aerobraking vehicle.

Parametric Uncertainties and Their Effects

In order to ascertain the robustness of the aerobraking maneuver, we numerically perturb the parameters for a specific example and observe the effect on the output variables. This method is simple

*Doctoral Candidate, School of Aeronautics and Astronautics.

†Associate Professor, School of Aeronautics and Astronautics. Associate Fellow AIAA. Member AAS.

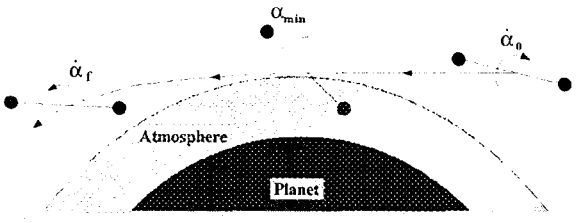

Fig. 2 Aerobraking maneuver.

and accurate, but it is limited to the specific problem at hand. However, attaining general expressions for the parametric sensitivities seems unlikely for such a complicated system.

The model used to simulate the tethered acrobraking maneuver was developed in Ref. 7. The tether is modeled as a rigid rod subjected to distributed aerodynamic and gravitational forces. The probe and orbiter are treated as particles. The atmosphere is assumed to be exponential and rotating with the planet.

For the nominal (baseline) maneuver, we achieve aerocapture at Mars into an orbit with a final eccentricity, e_f, of 0.50. (Arrival conditions at Mars are determined by a Hohmann transfer from Earth.) To ensure that the orbiter is not subjected to significant aerodynamic effects, we require the minimum altitude of the orbiter to be 14.5 km above the minimum altitude of the probe. This is referred to as the *clearance* constraint. The tether is assumed to be made of Hercules AS4 graphite with a tensile strength of 3.6 GN/m^2 and a density of 1800 kg/m^3. The optimal maneuver is obtained by mapping feasible solutions to locate a local minimum in the tether mass. (See Refs. 13 and 14 for a complete description of this process.) This maneuver is called *inclined* because the tether orientation is at an angle with respect to the local vertical (i.e. $\alpha_{min} \neq 0$ in Fig. 2) at periapsis (see Ref. 14 for more about maneuver types). The tether mass, length and diameter are

$$m_t = 411\ kg, \quad l_t = 38.8\ km, \quad d_t = 2.74\ mm \qquad (1)$$

whereas the propellant mass required for an equivalent ΔV (to capture the orbiter) is 571 kg.

The values of the input parameters that govern this case and their standard deviations are listed in Table 1. This list includes all the initial conditions and system properties used to simulate the maneuver except for the tether material properties which are assumed to be perfectly known. The uncertainties are based primarily upon the literature, but engineering judgement was required when references were unavailable. To illustrate the latter, consider that a small deviation in the spin rate yields a large error in orientation over a duration of several hours or more. Thus, some autonomous control (e.g. changing the tether length) is required to reduce this error. Since research in this area is scarce, a control error of 2 degrees was assumed as a conservative guess. In all cases, if standard deviations are not well known, the uncertainties were chosen so as to err on the conservative side.

The results of perturbing the input variables by one standard deviation are shown in Table 2. We are interested in the effect the perturbation has on the final eccentricity, e_f, the maximum tension exerted on the tether, T_{max}, and the clearance altitude the orbiter maintains above the probe, Δh. (These three output variables correspond to constraints on the final orbit, required cross-sectional area, and clearance.) These results show that the 1σ perturbations of the individual input variables do not have any catastrophic consequences on the aerobraking maneuver. None of the final eccentricities indicate a collision course with Mars ($e_f = 1.0$) nor an uncaptured orbit ($e_f \geq 1$). (Here we note that in the case of a crash, the time-varying eccentricity first plummets toward zero and then increases to a value of unity, indicating a degenerate orbit.) The worst case occurs at $\pm 50\%$ density, where e_f ranges from 0.27 to 0.79.

The largest increase in the nominal T_{max} is 26%, also due to the uncertainty associated with density. This causes the tether to break since the tether was only designed to withstand the nominal tension profile, but this can be corrected by building a safety factor into the design. To get an estimate for the extra mass required, note that the tether strength is proportional to mass. Thus, the ratio between the perturbed and nominal tension serves as an approximate ratio for the increase in tether mass, Δm, which is shown in Table 2. Assuming the perturbations are uncorrelated and linear, we can root sum square the mass perturbations to determine the total increase in mass necessary to accommodate the *system* 1σ uncertainty. This yields an approximate increase of 150 kg to bring the total tether mass to 560 kg.

The uncertainty in density also causes the greatest decrease in clearance from the baseline case. The minimum altitude of the orbiter is only 5.57 km above the probe, indicating that the orbiter would be subjected to significant heating. Again, we redesign the tether so this does not occur. An analogous approach to the strength matching performed above is to find a new tether length based on a ratio between the achieved and desired clearance. Unfortunately, the physics of the problem do not permit this method, since the clearance is not necessarily proportional to tether length. Thus, a new nominal maneuver must

Table 1. Parameter Uncertainties

Name	Variable	Mean Value	Uncertainty (1σ)	Comments
Orbiter Mass	m_o	1000 kg	50 kg	
Probe Mass	m_p	1000 kg	50 kg	
Tether Mass	m_t	410.5 kg	20 kg	
Orbiter Ballistic Coef.	$m_o/C_{Do}A_o$	100	33%	Based on Ref. 5
Probe Ballistic Coef.	$m_p/C_{Dp}A_p$	1.65	33%	Based on Ref. 5
Tether Drag Coef.	C_{Dt}	2	33%	Based on Ref. 5
Tether Length	l_t	38.8 km	0.4 km	Accounts for length uncertainty and stretching
Tether Diameter	d_t	2.74 mm	0.03 mm	
Gravitational Constant	μ_{eff}	42800 km^3/s^2	400 km^3/s^2	Accounts for model uncertainty in spherical harmonics
Target Altitude	$R_{peri} - R_{pl}$	81.7 km	2 km	Based on Ref. 12
Atmosphere Rotation	Ω	7.1 $\times 10^{-5}$ rad/s	50%	Accounts for wind variations
Density	ρ	0 - 6.3 $\times 10^{-6}$ kg/m^3	50%	Uncertainty is associated with the closest approach altitude. Based on Refs. 4,5,12
Initial Orientation Angle	α_o	284^o	2^o	Requires some autonomous S/C attitude control
Initial Spin Rate	$\dot{\alpha_o}$	-0.0159 rad/s	1 $\times 10^{-3} rad/s$	
Hyperbolic Excess Speed	V_{inf}	2.65 km/s	1 m/s	Based on Ref. 12

Table 2. Simulation Results for Parameter Uncertainties (1σ)

Variable	Perturbation	e_f	$T_{max}(N)$	$\Delta h(km)$	$\Delta m(kg)$
Nominal Case	0	0.5000 (0.5000)[a]	21105	14.50	0
Density	+50%	0.2653 (0.0104)	26542	5.57	105.76
	-50%	0.7910 (1.0165)	13977	14.03	0
Probe Ballistic Coef.	+ 33%	0.3654 (0.1543)	25261	8.56	80.85
	- 33%	0.6572 (0.8382)	16133	15.53	0
Target Altitude	+ 2 km	0.6194 (0.7260)	18192	14.69	0
	- 2 km	0.3603 (0.2045)	24357	8.28	63.26
Orbiter Mass	+ 50 kg	0.5119	21880	14.64	15.29
	- 50 kg	0.4878	20319	14.26	0
Atmos. Rotation Rate	$+3.6 \times 10^{-5}$ r/s	0.5293	20400	14.61	0
	-3.6×10^{-5} r/s	0.4698	21820	13.17	13.91
Probe Mass	+ 50 kg	0.5066 (0.5249)	20588	14.40	0
	- 50 kg	0.4938 (0.4738)	21639	13.73	10.39
Tether Drag	+ 33%	0.4827	20657	14.24	0
	- 33%	0.5171	21558	14.55	8.81
Spin Rate	+ 0.001 r/s	0.4448	21490	6.30	7.49
	- 0.001 r/s	0.5632	19928	9.59	0
Tether Length	+ 0.4 km	0.4942	21355	14.50	4.86
	- 0.4 km	0.5056	20857	14.45	0
Tether Mass	+ 20 kg	0.5059	21286	14.51	3.52
	- 20 kg	0.4938	20921	14.39	0
Gravitational Const.	+400 km^3/s^2	0.4989 (0.4952)	21219	14.28	2.22
	-400 km^3/s^2	0.5010 (0.5049)	20985	14.17	0
Orbiter Ballistic Coef.	+ 33%	0.4976	21084	14.48	0
	- 33%	0.5022	21125	14.49	0.40
Tether Diameter	+ 0.03 mm	0.4993	21090	14.49	0.29
	- 0.03 mm	0.5005	21120	14.50	0
Orientation	+ 2°	0.5060	21085	13.73	0
	- 2°	0.4939	21110	13.25	0.10
Hyp. Excess Speed	+ 1 m/s	0.5003 (0.5004)	21107	14.48	0.06
	- 1 m/s	0.4995 (0.4997)	21102	14.48	0

[a] Parentheses denote results for the ballistic vehicle.

be designed to achieve the clearance constraint. This is accomplished in the Preliminary Tether Design section.

A conventional ballistic vehicle is used as a metric by which to compare the sensitivity of the aerobraking tether. Using the same aerodynamic model as the tether system yields the following equations of motion for a single particle

$$\ddot{r} = -\mu/r^2 + r\dot{\theta}^2 - \frac{\rho\, C_D A \dot{r}}{2m}\sqrt{\dot{r}^2 + r^2(\dot{\theta} - \Omega)^2} \quad (2)$$

$$\ddot{\theta} = -2\dot{r}\dot{\theta}/r - \frac{\rho\, C_D A}{2m}\sqrt{\dot{r}^2 + r^2(\dot{\theta} - \Omega)^2} \quad (3)$$

where r and θ are the positional coordinates of the vehicle and the remaining parameters are given in Table 1. As before, perturbations of one standard deviation are applied to the nominal ($e_f = 0.50$) conventional maneuver for all relevant input variables. The only output that pertains to the ballistic vehicle is the final eccentricity. Results are given parenthetically in Table 2. The ballistic vehicle is shown to be much more sensitive to parameter uncertainties. The deviations in the atmospheric density cause the final orbit to range from nearly circular ($e_f = 0.01$) to hyperbolic ($e_f = 1.02$). The results are catastrophic for $+1\sigma$ variations because the vehicle fails to achieve capture.

Aerobraking Tether Robustness

The results above indicate that the tethered system provides some sort of inherent compensation for parameter variations that is not present in the conventional aerobraking vehicle (at least for the example under investigation). This is apparently due to the additional degree of freedom afforded by the rotation of the tether. Since the tether is initially spinning in the direction opposite the orbital rotation, the dynamics that result seem to serve as a self-correcting mechanism for any off-nominal conditions.

To illustrate, suppose the atmosphere is 50% less dense than expected. This means that targeted altitude is too high and the ensuing drag force (which is mostly on the probe) is insufficient. However, this also means the that drag torque is less than it would be for the nominal trajectory so it takes more time for the spin rate to reach zero. As a result, the tether is more vertical (α_{min} is smaller) than it would be nominally and the probe achieves a *lower* altitude than was targeted. (Note that the center of mass altitude is higher than the nominal trajectory, but not enough to offset this effect.) This is illustrated in Fig. 3 where the probe altitude for the -50% density perturbation reaches a minimum altitude about 2 *km* lower than

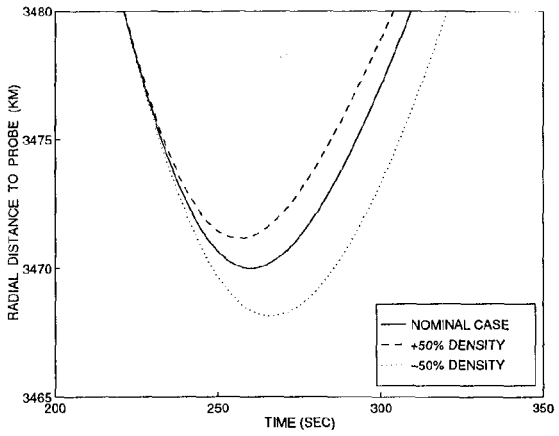

Fig. 3 Radial distance to the probe (tethered system).

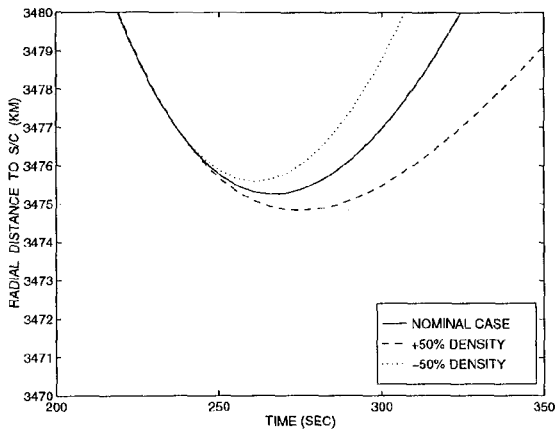

Fig. 4 Radial distance to the ballistic vehicle (opposite trend to Fig. 3).

the nominal. Conversely, if the atmosphere is more dense than the nominal, the tether does not "dip" as deeply into the atmosphere, as shown in the trajectory for the +50% density of Fig. 3.

The ballistic vehicle, on the other hand, has the opposite behavior. When the atmospheric density is less than expected, the orbit decays less than the nominal maneuver and the vehicle flies through a higher altitude as shown in Fig. 4. Thus, the achieved ΔV is lower for two reasons – a lower density is encountered and the periapsis radius increases. The converse is also true if a higher density is present at Mars.

Preliminary Tether Design

Due to the probabilistic nature of the parameter uncertainties, performance of the tether system cannot be accurately assessed by propagating one or even a handful of cases. Thus, Monte Carlo simulations are used for evaluation, where input parameters are generated according to their probability densities. Our goal is to design a maneuver (and a tether) so that constraints on final eccentricity, clearance and tether strength will be satisfied within at least one standard deviation of the mean for the respective outputs.

As mentioned above, redesigning the tether so that it can achieve the required clearance for 1σ perturbations cannot be accomplished by merely changing the tether length. A new nominal maneuver is required with sufficient clearance to accommodate the parameter uncertainties to within one standard deviation. To determine a "sufficient" nominal clearance, a root sum square of the amount by which the clearance constraint was violated for all the cases in Table 2 can be used to obtain a scale factor. This, however, yields a negative clearance, which indicates that no amount of clearance in the nominal maneuver is adequate for 1σ certainty. Alternatively, in the hope that the RSS value is conservative, the worst case (density) is used to calculate a new clearance. By scaling the desired clearance, 14.5 km, by the ratio between the desired and achieved clearance for the +50% density case we estimate

$$\Delta h_{est} = \frac{14.5}{5.57}(14.5\ km) = 37.7\ km \qquad (4)$$

Rounding this number conservatively yields a new nominal clearance of 40 km. After some computations, the optimal maneuver for $e_f = 0.50$ and $\Delta h = 40\ km$ is found to have the following characteristics:

$$m_t = 654\ km,\quad l_t = 97.6\ km,\quad d_t = 2.18\ mm \qquad (5)$$

This new nominal is called a *vertical maneuver*[14] because the tether is nearly aligned with the local vertical at periapsis ($\alpha_{min} \approx 0$). The minimum tension in the tether, T_{min}, is nearly zero for this type of maneuver as shown in Table 3.

We now perturb the input variables by one standard deviation as we did with the original nominal to get a rough idea of the system performance. The corresponding changes in the output variables are listed in Table 3. This preliminary design is based only upon the uncertainty in density, probe ballistic coefficient, target altitude and initial spin rate, since the changes in the maximum tension and clearance for these parameters greatly exceed the others.

The new nominal maneuver has two advantages. First of all, we note from Table 3 that the clearance constraint is not violated when the new nominal is perturbed (i.e. $\Delta h > 14.5\ km$). Secondly, the aerobraking tether is even more robust (in terms of final eccentricity) than the previous case as evidenced by a narrower band of final eccentricities. (There is, however, a bias present.) Unfortunately, the minimum tension has dropped below zero in some cases, which could have deleterious effects since the tether cannot support compressive forces.

This design was iterated upon (using optimization software and Monte Carlo techniques) to minimize these compressive forces and to strengthen the tether so that the perturbations would not cause it to break. The characteristics of the final (preliminary) design are

$$m_t = 1470\ kg,\quad l_t = 126\ km,\quad d_t = 2.89\ mm \qquad (6)$$

One thousand simulations of the design were performed with input perturbations generated by MATLAB for an assumed normal distribution with associated standard deviations listed in Table 1.

Histograms from the Monte Carlo simulation are shown in Figs. 5 – 8. The mean value, μ, of 0.665 for e_f (see Fig. 5) is biased higher than the original target of 0.50, but within one standard deviation (0.285), all the cases are captured. Of the thousand simulations, 120 were not captured and only one of the perturbed cases causes the system to crash into Mars. The results were equally successful for the maximum force, which is plotted in Fig. 6. The maximum allowable tether force for the diameter given in Eq. (6) is 23,400 N. Thus, to within a 1σ range of the mean, all the cases have an acceptable maximum force. The tether breaks in 165 of the cases shown. Also, the constraint on clearance, shown in Fig. 7, is satisfied within $\pm 1\sigma$ of the mean. The clearance of 110 cases was less than the desired value of 14.5 km, resulting in larger aerodynamic effects than deemed acceptable. The only constraint not satisfied for a 1σ range is that the minimum tension be greater than zero. In Fig. 8, the minimum tension $\mu - \sigma$ (2850 N − 2920 N) is slightly less than zero. A total of 177 cases have compressive forces. In all, there are 436 cases out of the 1000 simulations that violate at least one of the four constraints depicted in Figs. 5 – 8.

A Monte Carlo simulation is also performed for the ballistic vehicle for comparison. The same perturbations (for 1000 cases) used above are input into the ballistic vehicle equations. A histogram of the final eccentricity is shown in Fig. 9. Again, we see a much wider deviation on e_f ($\sigma = 0.48$) than achieved by

Table 3. Simulation Results for New Nominal Tether (1σ)

Variable	Perturbation	e_f	$T_{max}(N)$	$T_{min}(N)$	$\Delta h(km)$	$\Delta m(kg)$
Nominal Case	0	0.5000	13381	14	40.0	0
Density	+50%	0.4274	17169	2146	17.41	185
	−50%	0.8386	12717	-2456	83.32	0
Probe Ballistic Coef.	+ 33%	0.4514	16186	1410	23.37	137
	− 33%	0.6121	12870	-1973	83.75	0
Target Altitude	+ 2 km	0.5726	13107	-1222	69.37	0
	− 2 km	0.4464	16344	1044	22.95	145
Spin Rate	+ 0.001 r/s	0.4280	15952	-3003	31.29	126
	0.001 r/s	0.5769	12385	1805	56.23	0

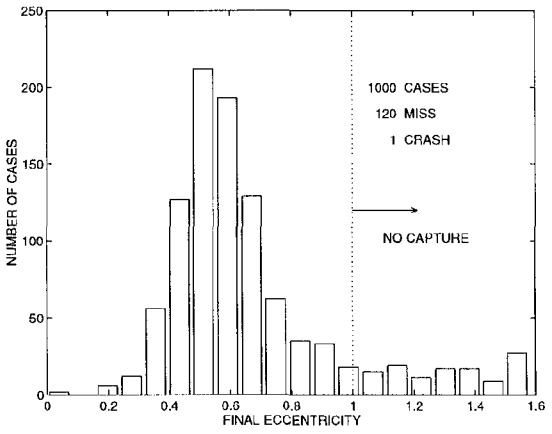

Fig. 5 Distribution of e_f for the aerobraking tether ($\mu = 0.665, \sigma = 0.285$).

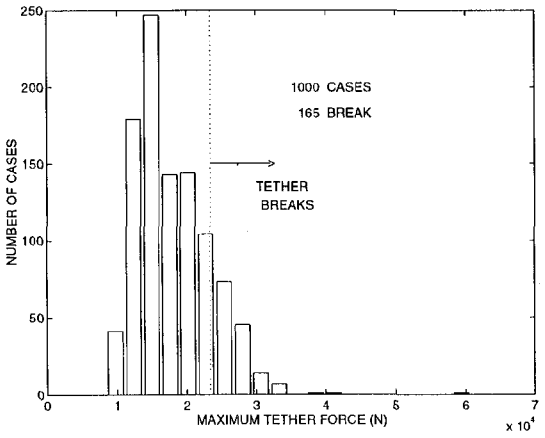

Fig. 6 Distribution of F_{max} for the tether ($\mu = 18000N, \sigma = 5340N$).

the tethered system. The number of crashes grows to 228 and the number of cases that do not achieve aerocapture increases to 230.

Assuming that violation of *any one* of the constraints constitutes a mission failure, the tether system has a 56% probability of success based on the Monte Carlo results. This is comparable to the success rate of 54% for the ballistic vehicle, which only has one constraint (final eccentricity). However, we note that the design is preliminary and represents a suboptimal result. Furthermore, violation of the constraints does not necessarily mean failure of the system; the actual success rate for the tethered system may be higher than indicated.

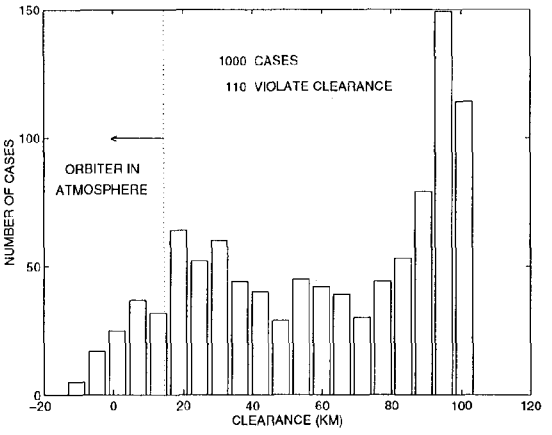

Fig. 7 Distribution of Δh for the tether ($\mu = 59.7km, \sigma = 33.5km$).

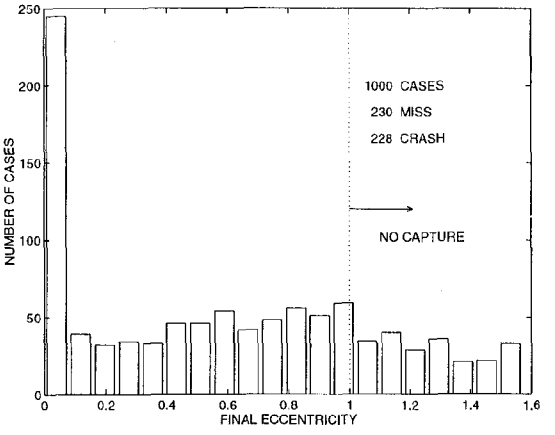

Fig. 9 Distribution of e_f for the ballistic vehicle ($\mu = 0.598, \sigma = 0.483$).

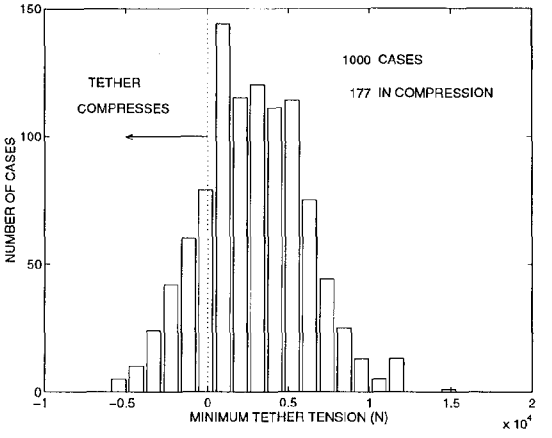

Fig. 8 Distribution of T_{min} for the tether ($\mu = 2840N, \sigma = 3240N$).

Future Work

The work presented here is by no means complete, but suggests several possibilities for further study.

1) Investigate constraint violations

Further simulation with more complicated (e.g. flexible) models must be performed to more accurately assess which constraint violations are actual mission failures. For example, a break in the tether may not be catastrophic if the orbiter remains captured and the probe is in a degenerate orbit.

2) Introduce a heating constraint

The clearance constraint employed above may not be the most useful criterion for design. A similar analysis can be performed by setting a maximum heating condition on the orbiter.

3) Enhance the inherent tether robustness

The design algorithm above uses mass optimal maneuvers for the nominal. This, however, may not be the most efficient maneuver when considering the parameter uncertainties. Higher spin rates, for example, may amplify the self-correcting nature of the tethered system.

4) Refine the tether design

More effective design tools, such as an analytic theory or an alternative algorithm for finding nominal maneuvers that somehow incorporates the statistical variations, could be developed so that a maneuver can be found that achieves all the constraints with a better probability of success.

5) Investigate control schemes

To reduce the tether mass, a feedback control scheme could be developed. A simple candidate is to change the tether length to control the altitude of the probe. Controllers applicable to the ballistic vehicle, such as changing the probe area or using a lifting body, are also possible. A related option is to take atmospheric measurements before entering the atmosphere (by using remote sensing or by sending a probe ahead of the spacecraft) and to adjust the spacecraft states accordingly.

6) Perform mission design

The resuable nature of the tether makes it an attractive alternative for mission design. A piloted Mars mission design, for example, can possibly use the same tether for orbit insertion[15], artificial gravity[16] and aerobraking. In a robotic mission,

the tether can also be used to attain science goals (e.g. dust collection from the Martian atmosphere for sample return[17]).

Conclusion

The aerobraking tether is shown to achieve reasonable robustness for parameter uncertainties. In terms of final eccentricity, the aerobraking tether is less sensitive to parametric uncertainties than the ballistic vehicle. To withstand the effects of uncertainties on other tether constraints, however, the tether must be massive. We expect that the size of the tether could be greatly reduced by a more refined design or an increase in strength of materials.

References

[1] Seiff, A., "Atmospheres of Earth, Mars, and Venus, as Defined by Entry Probe Experiments," *Journal of Spacecraft and Rockets*, Vol. 28, No. 3, 1991, pp.265-275.

[2] Culp, R.D. and Stewart, A.I., "Time-Dependent Model of the Martian Atmosphere for Use in Orbit Lifetime and Sustenance Studies," *The Journal of the Astronautical Sciences*, Vol. 32, No.3, pp. 329-341.

[3] Lyons, D.T., "Aerobraking: The Key to Affordable Mars Exploration," IAA-L-0512, *Second IAA (International Academy of Astronautics) International Conference on Low-Cost Planetary Missions*, Laurel, MD, 1996.

[4] Gurley, J.G., "Guidance for an Aerocapture Maneuver," *Journal of Guidance, Control, and Dynamics*, Vol. 16, No. 3, 1993, pp. 505-510.

[5] Shipley, B.W. and Ward, D.T., "Robust Control Algorithms for Mars Aerobraking," *Advances in the Astronautical Sciences*, Vol. 79, 1992, pp. 633-652.

[6] Braun, R.D. and Powell, R.W., "Predictor-Corrector Algorithm for Use in High-Energy Aerobraking System Studies," *Journal of Guidance, Control, and Dynamics*, Vol. 15, No. 3, 1992, pp. 672-678.

[7] Puig-Suari, J. and Longuski, J.M., "Modeling and Analysis of Orbiting Tethers in an Atmosphere," *Acta Astronautica*, Vol. 25, No. 11, 1991, pp. 679-686.

[8] Puig-Suari, J., Longuski, J.M., and Tragesser, S.G., "A Three Dimensional Hinged-Rod Model for Flexible-Elastic Aerobraking Tethers," AAS 93-730, *AAS/AIAA Astrodynamics Specialist Conference*, Victoria, B.C., 1993.

[9] Longuski, J.M., Puig-Suari, J., and Mechalas, J., "Aerobraking Tethers for the Exploration of the Solar System," *Acta Astronautica*, Vol. 35, No. 2/3, 1995, pp. 205-214.

[10] Puig-Suari, J., Longuski, J.M., and Tragesser, S.G., "Aerocapture with a Flexible Tether," *Journal of Guidance, Control, and Dynamics*, Vol. 18, No. 6, 1995, pp. 1305-1312.

[11] Longuski, J.M., Puig-Suari, J., Tsiotras, P., and Tragesser, S.G., "Optimal Mass for Aerobraking Tethers," *Acta Astronautica*, Vol. 35, No. 8, 1995, pp. 489-500.

[12] McEneaney, W. M. and Mease, K. D., "Error Analysis for a Guided Mars Landing," *The Journal of the Astronautical Sciences*, Vol. 39, No. 4, 1991, pp. 423-445.

[13] Tragesser, S.G., Longuski, J.M., Puig-Suari, J., and Mechalas, J.P., "Analysis of the Optimal Mass Problem for Aerobraking Tethers," AIAA-94-3747, *AIAA/AAS Astrodynamics Conference*, Scottsdale, AZ, 1994.

[14] Tragesser, S.G., Longuski, J.M. and Puig-Suari, J., "A General Approach to Aerobraking Tether Design," AAS 95-353, *AAS/AIAA Astrodynamics Specialist Conference*, Halifax, Nova Scotia, 1995.

[15] Puig-Suari, J., Longuski, J.M., and Tragesser, S.G., "A Tether Sling for Lunar and Interplanetary Exploration," *Acta Astronautica*, Vol. 36, No. 6, 1995, pp. 291-296.

[16] Kowalsky, C. and Powell, J.D., "Tethered Artificial Gravity Spacecraft Design," AAS 93-701, *AAS/AIAA Astrodynamics Specialist Conference*, Victoria, B.C., 1993.

[17] Pasca, M. and Lorenzini, E., "Optimization of a Low Altitude Tethered Probe for Martian Atmosphere Dust Collection," *Proceedings of the 4th International Conference on Tethers in Space*, Washington, D.C., Vol. 3, 1995, pp. 1663-1674.